Available online at www.sciencedirect.com
SCIENCE DIRECT
Journal of Power Sources 148 (2005) 66–71
JOURNAL OF POWER SOURCES
www.elsevier.com/locate/jpowsour

Electrochemical performance of nanocrystalline $LiMPO_4$ thin-films prepared by electrostatic spray deposition

Jun Ma, Qi-Zong Qin *

Department of Chemistry, Laser Chemistry Institute, Fudan University, Shanghai 200433, PR China

Received 8 November 2004; received in revised form 14 December 2004; accepted 25 January 2005
Available online 2 April 2005

Abstract

$LiMPO_4$ (M = Mn, Fe) and $LiMn_{0.4}Fe_{0.6}PO_4$ thin-films have been fabricated by electrostatic spray deposition (ESD) combined with sol–gel method, in which P_2O_5 was used as a phosphorous resource in Li–M–P–O alcohol precursor solution. Analyses of $LiMPO_4$ solid films using X-ray diffractometry (XRD) and scanning electron microscopy (SEM) demonstrated the formation of an olivine phase of space group *Pmnb* with nanocrystalline morphology. The prepared $LiMPO_4$ films were evaluated electrochemically by cyclic-voltammetry and charge/discharge measurements. The results showed that thin-film electrode of $LiMn_{0.4}Fe_{0.6}PO_4$ exhibited better electrochemical performance than that of pure $LiFePO_4$ and $LiMnPO_4$.

Keywords: Electrostatic spray deposition; Lithium metal olivine phosphate; Thin-film; Lithium ion battery

1. Introduction

Lithium transition metal phosphates with ordered olivine structure $LiMPO_4$ (M = Mn, Fe, Co and Ni) have attracted much attention as promising new cathode materials for rechargeable lithium batteries since the pioneering study on $LiFePO_4$ by Padhi et al. [1]. To our knowledge, the conventional method for the synthesis of metal olivine phosphates involves the use of high-temperature solid-state reactions in Ar ambient to achieve a powder product for use as cathode materials, but this method includes many complex steps for a long time and consumes a large amount of energy and inert gas [2]. Recently, many wet-chemical methods, such as sol–gel method [3–7] and direct precipitation route [8] were successfully developed to optimize new synthetic routes of $LiMPO_4$ and improve their electrochemical performance. Scrosati and co-workers [3] provided a novel aspect based on a critical step involving the dispersion of metal (Cu or Ag) at a very low concentration in the precursor sol to synthesize $LiFePO_4$ powder and improve its capacity delivery and life cycle. Doeff and co-workers [5] prepared $LiFePO_4$ by sol–gel method and incorporated organic additives to form conductive carbon-coating on $LiFePO_4$ particles to improve its energy density. Recently, Tarascon and co-workers [8] reported a one-step low-temperature route to precipitate the $LiMnPO_4$ powder from a homogeneous solution. Besides $LiMPO_4$ powders, there are several reports on the preparation of the olivine $LiMPO_4$ thin-films by physical deposition methods. Both Ogumi and co-workers [9] and Tarascon and co-workers [10] employed pulsed laser deposition (PLD) to fabricate well-crystallized $LiFePO_4$ thin-films and formed typical features of olivine $LiFePO_4$ film cathodes. Additionally, West et al. [11] and Eftekhari [12] prepared $LiCoPO_4$ and $Al_2O_3/LiCoPO_4$ thin-films using rf sputtering technique, respectively, and obtained the anodic and cathodic peaks of Co^{3+}/Co^{2+} couple at 4.8 V in cyclic-voltammetry tests. However, these olivine thin-film cathodes exhibited a low capacity, mainly due to their poor electronic conductivity.

In this paper, we developed a new fabrication method involving electrostatic spray deposition (ESD) technique combined with sol–gel process to simplify the fabrication route

* Corresponding author. Fax: +86 2165102777.
E-mail address: qzqin@fudan.ac.cn (Q.-Z. Qin).

0378-7753/$ – see front matter © 2005 Elsevier B.V. All rights reserved.
doi:10.1016/j.jpowsour.2005.01.041

of olivine phosphate $LiMPO_4$ thin-films. Since ESD method offers many advantages for thin-film deposition, such as low cost set-up, high deposition efficiency and easy control of composition of the deposited films, many conventional cathode thin-films for lithium rechargeable batteries, e.g. $LiCoO_2$ [13], $LiMn_2O_4$ [14], $LiNiO_2$ [15] and V_2O_5 [16] have been successfully prepared by this method. However, there is no report on lithium transition metal phosphate thin-films prepared using ESD. A typical ESD method usually requires to prepare a precursor solution, which is composed of lithium salts, transition metal salts and phosphoric acid as Li, M and PO_4^{3-} resources, respectively. Because of the insolubility of metal phosphate in alcohol, we tried to disperse P_2O_5 as the phosphorous resource into the prepared Li–M–P–O solution with much higher concentration. The motivation of this work is to fabricate the olivine $LiFePO_4$, $LiMnPO_4$, and $LiMn_yFe_{1-y}PO_4$ thin-films by using modified ESD method, and to examine the correlation of key experimental conditions for the $LiMPO_4$ preparation with the electrochemical performance of these thin-film cathodes in lithium batteries.

2. Experimental

To prepare a Li–M–P–O solution used for ESD, a stoichiometric amount of analytical grade $LiNO_3$ and metal salts $M(NO_3)_m{\cdot}nH_2O$ (M = Fe, Mn) with the cationic ratio of Li:M = 1:1 were dissolved in a mixed solvent of absolute ethanol:glycol:butyl carbitol ($CH_3(CH_2)_3O(CH_2)_2O(CH_2)_2OH$, 85%) with volume ratio of 4:1:1 to form a transparent Li–M–O sol. Here butyl carbitol can be effective in maintaining a uniform film [17]. P_2O_5 powders dissolved in a mixed solvent of H_2O:ethanol with volume ratio of 1:2 was used as a phosphorous resource. After mixed the Li–M–O sol and P_2O_5 solution, a homogeneous precursor solution of 0.02 M with element ratio of Li:M:P = 1:1:1 was obtained. For the preparation of Li–Fe–P–O solution, we added excessive amount of ascorbic acid to reduce Fe^{3+} to Fe^{2+} [3].

A detailed description of the ESD set-up used in this work has been presented elsewhere [17,18]. Briefly, a positive voltage of 8.0 kV from a direct current (dc) power supply was applied to a stainless steel nozzle of a syringe to generate an aerosol. The nozzle–substrate distance was fixed at 3.0 cm. A syringe pump with a definite flowing rate was used to pump the precursor solution. A stainless steel foil (1.5 cm × 1.0 cm) was used as a substrate and weighed before and after the deposition to estimate the weight of deposited film. The deposition time is dependent on the required film thickness and the flowing rate of the precursor solution. The film deposition was carried out at a substrate temperature of 120 °C.

The sample deposited on the substrate by ESD was calcinated at 500–750 °C for 2 h under pure Ar ambient. The temperature was controlled at a stable ascending rate of 5 °C min^{-1} and the sample was cooled with flowing pure Ar.

The structure and phases of the $LiMPO_4$ thin-film samples were identified by X-ray diffractometry (XRD) (Rigata/Max-C diffractometer with Cu $K\alpha_1$ source). The morphology and component of the thin-film samples was recorded by using a scanning electron microscopy (SEM) (Cambridge S-360) coupled with an energy dispersed X-ray (EDX) analysis.

An electrochemical cell was constructed by using the thin-film electrode as the working electrode, and two lithium foils as a counter electrode and a reference electrode, respectively. The electrolyte consisted of 1 M $LiPF_6$ dissolved in a non-aqueous solution of ethylene carbonate (EC) and dimethyl carbonate (DMC) with a weight ratio of 1:1. All the cells were assembled in an argon-filled glove box. Cells were cycled at a constant current using a LAND BT 1-40 battery test system. Cyclic-voltammetry (CV) measurements were carried out by using a CHI 660a electrochemical working station (CHI Instruments, TN).

3. Results and discussion

3.1. Film characterization

XRD patterns of $LiFePO_4$ and $LiMnPO_4$ films deposited on stainless steels calcinated at different temperature in Ar ambient are presented in Figs. 1 and 2. As shown in Fig. 1, the diffraction peak at 50.8° is attributed to the stainless steel substrate, and main diffraction peaks can be indexed in the D_{2h}^{16} space group *Pmnb*. The lattice parameters of well-crystallized $LiFePO_4$ are $a = 6.019$ Å, $b = 10.347$ Å and $c = 4.704$ Å, according to the JCPDS (77-0179). It is obvious that the olivine phase of $LiFePO_4$ begins to appear at the calcinated temperature of 600 °C, and well formed at higher temperatures. It should be noted that the peaks of $LiFePO_4$ become sharper and the Fe_2O_3 peaks appear to be clear when the film sample was calcinated at 700 °C. This result is similar to the previous reports on the XRD patterns of $LiFePO_4$ powder prepared by the conventional synthetic methods [5,19]. It implies that the presence of small amount of impurity phase Fe_2O_3 could not be eliminated completely

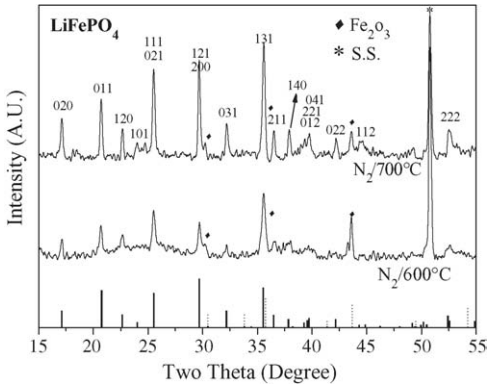

Fig. 1. X-ray diffraction (XRD) pattern of $LiFePO_4$ films calcinated at 600 and 700 °C in Ar ambient.

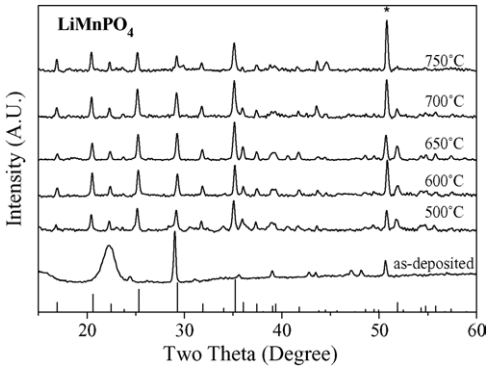

Fig. 2. X-ray diffraction (XRD) pattern of $LiMnPO_4$ films calcinated at different temperatures Ar ambient.

at the calcinated temperature higher than 600 °C. The primary crystallite size was estimated by measuring the width of the strongest diffraction peak and using Scherrer equation. Typically, the average crystalline size of $LiFePO_4$ thin-film calcinated at 700 °C was formed to be around 35 nm, indicating that a nanocrystalline structure of the $LiFePO_4$ film was formed.

Fig. 2 shows the XRD patterns of $LiMnPO_4$ thin-films as a function of the calcinating temperature in Ar ambient. It can be seen that the as-deposited $LiMnPO_4$ film prepared by ESD at substrate temperature of 120 °C appears some broad and sharp diffraction peaks, which cannot be attributed to the olivine structure of $LiMnPO_4$. When the $LiMnPO_4$ thin-films were calcinated at a temperature >500 °C, the olivine structure of $LiMnPO_4$ was demonstrated by measured XRD patterns, in which more than 20 reflections can be indexed in the *Pmnb* space group with the following lattice parameters ($a = 6.1061$ Å, $b = 10.4521$ Å and $c = 4.7461$ Å), in agreement with a well crystalline single phase $LiMnPO_4$ according to the JCPDS [20]. As shown in Fig. 2, all of these XRD patterns for the film samples calcinated at the temperatures higher than 500 °C were nearly the same as those of the powder samples reported previously [21]. Different from the $LiFePO_4$ film sample mentioned above, no impurities were determined with the XRD results.

It is well known that the morphology of the $LiFePO_4$ film depended on the deposition conditions such as feeding rate, precursor solution, and the voltage between nozzle and substrate. SEM micrographs of the $LiFePO_4$ thin-films calcinated at 700 °C deposited at different feeding rates are presented in Fig. 3. It can be seen that the grain size of the $LiFePO_4$ films decreased with decreasing the feeding rate of the precursor solution in the ESD process. The $LiFePO_4$ film deposited at a feeding rate of 0.5 mL h^{-1} showed a blossom-like morphology with a large particle size (>400 nm) (Fig. 3(a)). When the feeding rate decreased to 0.05 mL h^{-1}, the deposited $LiFePO_4$ thin-film appeared to be much uniform, and the average particle size became smaller and was estimated to be less

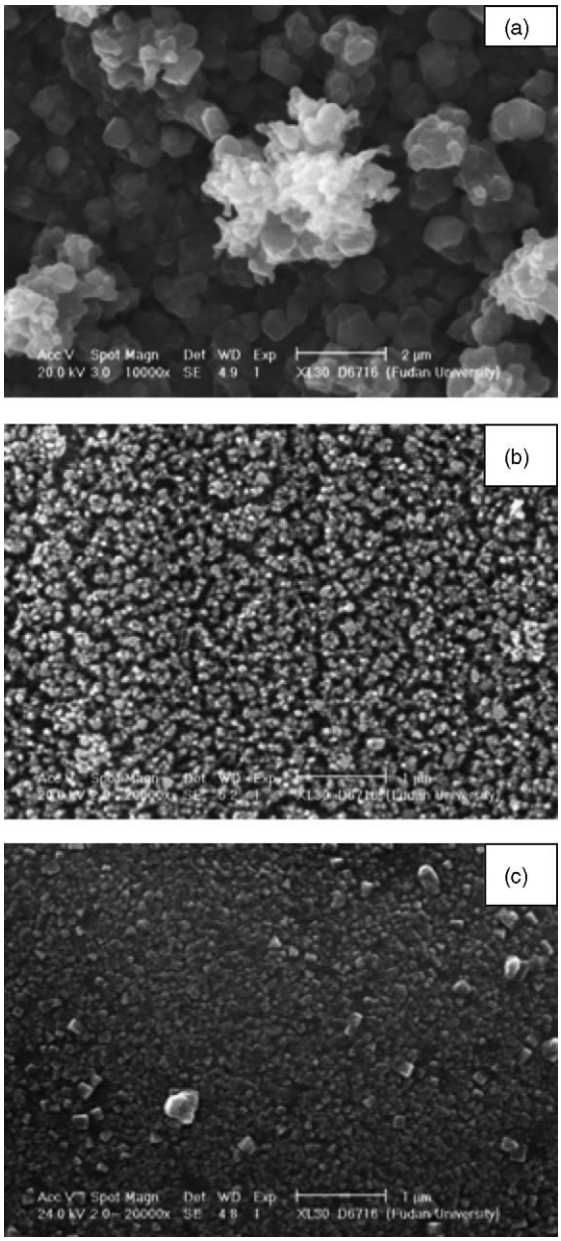

Fig. 3. SEM photographs of $LiMPO_4$ films. (a) $LiFePO_4$ deposited at 0.5 mL h^{-1} rate and calcinated at 700 °C; (b) $LiFePO_4$ deposited at 0.05 mL h^{-1} rate and calcinated at 700 °C; (c) $LiMnPO_4$ deposited 0.05 mL h^{-1} rate and calcinated at 600 °C.

than 100 nm (Fig. 3(b)). The main reason may be that the precursor droplet pumped from nozzle at high feeding rates could not be dispersed completely before deposited onto the substrate, and crystallized to large grains through calcinations. The SEM images of the $LiMnPO_4$ film calcinated at 600 °C as shown in Fig. 3(c) presented uniform particle size and dense surface, and the grain size was estimated to be ~50 nm. The elemental analysis performed by EDX showed a molar ratio of about 1:1.2:4.4 for Mn:P:O, which is close to the stoichiometric composition of $LiMnPO_4$.

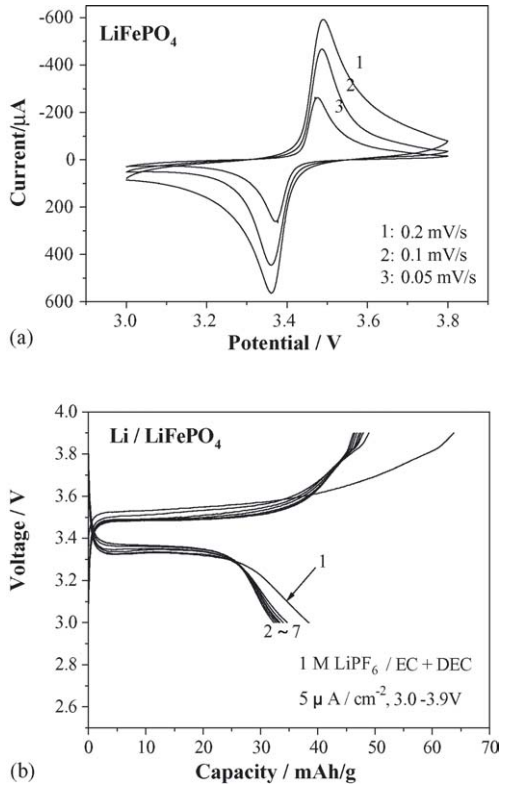

Fig. 4. (a) Cyclic-voltammograms for $LiFePO_4$ film electrodes in 1 mol dm^{-3} $LiPF_6$/(EC + DEC) at different scan rates; (b) charge/discharge curves for $LiFePO_4$ film electrodes.

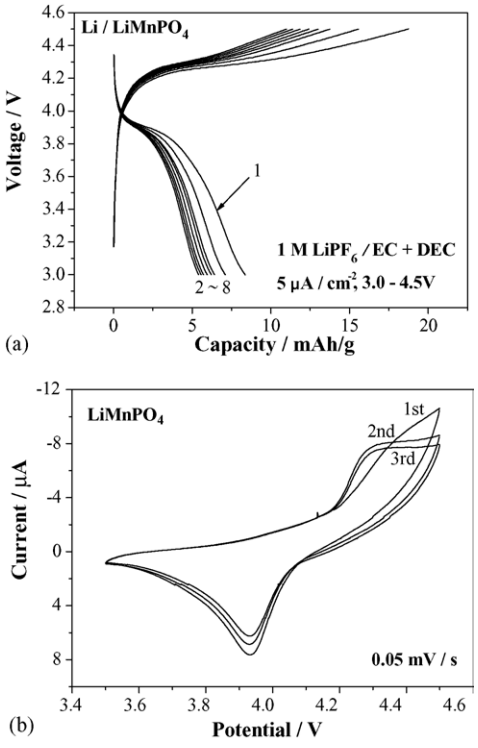

Fig. 5. (a) Charge/discharge curves for $LiMnPO_4$ film electrodes; (b) cyclic-voltammograms for $LiMnPO_4$ film electrodes in 1 mol dm^{-3} $LiPF_6$/(EC + DEC) at different scan rates.

3.2. Electrochemical performance

Cyclic-voltammograms (CVs) for $LiFePO_4$ film/$LiPF_6$ + EC + DMC/Li cell cycled between 3.0 and 3.9 V versus Li^+/Li at different scan rates are shown in Fig. 4(a). It can be seen that only a couple of anodic and cathodic peaks appear at 3.48 and 3.35 V, respectively, and there is no obvious difference for the peak positions in CV curves measured at different scan rates. However, the difference between the peak potentials ΔE_p is relatively high and estimated to be about 130 mV. It implies that there are some kinetic limitations during electrochemical processes. This well-defined redox peaks corresponding to the Fe^{2+}/Fe^{3+} couple is the characteristic of $LiFePO_4$. The mean redox potential is 3.41 V, which is well in agreement with the previous results [3], indicating the typical feature of $LiFePO_4$ cathode can be obtained for the thin-film prepared by ESD method. The typical charge/discharge curves for a $LiFePO_4$ film electrode prepared by ESD and calcinated at 700 °C are presented in Fig. 4(b). It can be seen that the charge/discharge plateaus are found to be ~3.48 and ~3.35 V, respectively, which are well in agreement with the CV result in Fig. 4(a). The open circuit voltage of $LiFePO_4$ film/Li cell is found to be ~3.2 V. Upon charging and discharging, the initial charge capacity until the cut-off voltage of 3.8 V is estimated to be ~65 mAh g^{-1}, and the initial discharge capacity is ~40 mAh g^{-1}. The coulombic efficiency is obtained to be 60%, and increased to 75% after the seventh cycle. Although the specific capacity of the $LiFePO_4$ film is not as good as its powder form reported previously [4], our result is better than that of $LiFePO_4$ films prepared by PLD method [10]. The observed irreversible capacity could be due to the poor electronic conductivity of the active olivine materials, and a part of Fe(II) oxidized to Fe(III).

Different from the $LiFePO_4$, the electrochemical activity of $LiMnPO_4$ powders used as a cathode material in lithium cell is still a controversial debate. Padhi et al. [1] and Okada et al. [22] were unable to extract any lithium from $LiMnPO_4$, but a reversible capacity of 140 mAh g^{-1} was achieved for the solid-state synthesized $LiMnPO_4$ powder reported by Li et al. [21]. Recently, the $LiMnPO_4$ powder prepared by a direct precipitation route from aqueous solution by Tarascon and co-workers [8] showed that only a low lithium extraction/insertion capacity of 70 mAh g^{-1} was obtained for pure $LiMnPO_4$. We also obtained the electrochemical activity of $LiMnPO_4$ thin-films deposited by ESD and calcinated at 600 °C, which was much lower than that of $LiFePO_4$ thin-film mentioned above. Fig. 5(a) shows the charge/discharge curves for $LiMnPO_4$/Li cell. Both first charge and discharge capacities were found to be ~20 mAh g^{-1}. However, the observed charge/discharge plateaus at 4.2/3.9 V were closed to those reported by Li et al. [21], and demonstrated the electrochemical characteristics of $LiMnPO_4$ thin-films. The CV curves in Fig. 5(b) shows that the anodic peak at 4.35 V

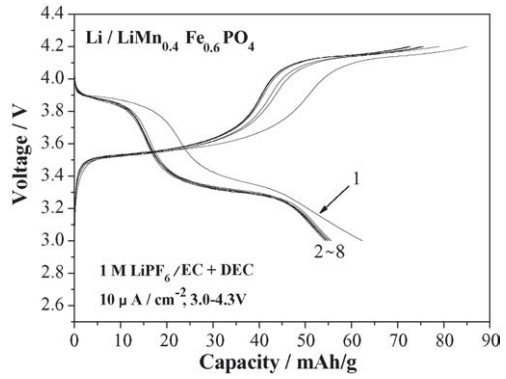

Fig. 6. Charge/discharge curves for $LiMn_{0.4}Fe_{0.6}PO_4$ film electrodes.

in the first cycle is slightly different from that in the subsequent cycles, while the cathodic peak was observed at 3.95 V during the anodic scan in the first three cycles. Upon cycling, the anodic peak potentials decreased slightly to 4.30 V. The difference of the peak separations between the anodic and cathodic peaks ΔE_p was estimated to be 300 mV, indicating a strong polarization and irreversible behavior during a $LiMnPO_4$ film/Li cell cycling. Our XRD results have showed that an olivine $LiMnPO_4$ thin-film can be obtained at various calcinated temperatures, but the electrochemical performance of $LiMnPO_4$ film electrode depends on the calcinated temperature. It has been demonstrated that the $LiMnPO_4$ films calcinated at 600 °C exhibited better performance than the film samples calcinated at other temperature.

In order to improve the electrochemical performance of pure $LiFePO_4$ and $LiMnPO_4$, the solid solution of $LiFe_yMn_{1-y}PO_4$ cathode has been investigated by some research groups [23–25]. The carbon-containing $LiFe_yMn_{1-y}PO_4$ compounds reported by Li et al. could achieve a capacity as high as 164 mAh g^{-1} as $y = 0.75$. According to this result, we prepared the $LiFe_yMn_{1-y}PO_4$ thin-films by mixing stoichiometric amount of Fe/Mn in the preparation of Li–Mn–Fe–P–O precursor solutions and used ESD method to deposit the thin-films. Their electrochemical behaviors were examined via charge/discharge measurements. Among them, the electrochemical performance of $LiMn_{0.4}Fe_{0.6}PO_4$ thin-film was the best one. The charge/discharge curves of the $LiFe_{0.6}Mn_{0.4}PO_4$ are shown in Fig. 6. It is clear that two charge/discharge plateaus at 4.3/4.1 and 3.5/3.35 V correspond to Mn^{3+}/Mn^{2+} and Fe^{3+}/Fe^{2+} redox couple, respectively, which is inconsistent with the potential positions of the redox couples reported previously [23]. The initial capacity of the $LiFe_{0.6}Mn_{0.4}PO_4$ was found to be about 70/55 mAh g^{-1}, which is higher than that of $LiFePO_4$ film. It is noted that the ratio of the capacity corresponding to Mn^{3+}/Mn^{2+} and Fe^{3+}/Fe^{2+} is estimated to be about 4:6, which is nearly the same as the metallic element ratio of Mn and Fe. The existence of Mn^{2+} ions could enhance the charge/discharge capacity of $LiFe_yMn_{1-y}PO_4$ [1]. However, the effect of the Fe/Mn ratio and calcinated temperature of $LiFe_yMn_{1-y}PO_4$ thin-films on their electrochemical performance is complicated, more works are in progress.

4. Conclusion

Thin-films of $LiMPO_4$ (M = Mn and Fe) and $LiFe_{0.6}Mn_{0.4}PO_4$ were fabricated successfully for the first time by ESD combined with sol–gel method. XRD results revealed that the crystal phase of these thin-films was an olivine structure indexed by orthorhombic *Pmnb*. SEM images showed that all the $LiMPO_4$ (M = Mn and Fe) films have a uniform surface morphology with average grain size less than 100 nm. The electrochemical performance of the $LiFePO_4$ and $LiMnPO_4$ thin-film electrodes demonstrated that both $LiFePO_4$ and $LiMnPO_4$ films exhibited typical features of those powder electrode reported previously. The $LiFe_{0.6}Mn_{0.4}PO_4$ film electrode exhibited a larger capacity than the pure $LiFePO_4$ and $LiMnPO_4$ film electrodes. Work in our laboratory is in progress to enhance the conductive properties of those olivine $LiMPO_4$ thin-films and improve their electrochemical performance. As a simple technique based on chemical deposition, ESD could be a promising method for the fabrication of functional ceramic thin-films in the use of thin-film lithium ion batteries.

Acknowledgement

This work was supported by the National Nature Science Foundation of China (Projects No. 20083001 and 20203006). The authors would like to thank Dr. Zheng-wen Fu very much for his valuable discussion.

References

[1] A.K. Padhi, K.S. Nanjundaswamy, J.B. Goodenough, J. Electrochem. Soc. 144 (1997) 1188.
[2] A. Yamada, et al., J. Power Sources 119–121 (2003) 232.
[3] F. Croce, A.D. Epifanio, J. Hassoun, A. Deptula, T. Olczac, B. Scrosati, Eletrochem. Solid-State Lett. 5 (3) (2002) A47.
[4] M.M. Doeff, Y.O. Hu, F. McLarnon, Eletrochem. Solid-State Lett. 6 (10) (2002) A207–A209.
[5] Y.O. Hu, M.M. Doeff, R. Kostecki, J. Electrochem. Soc. 151 (8) (2004) A1279.
[6] J.B. Lu, Z.T. Zhang, Z.L. Tang, W.C. Shen, Y.X. Xu, Rare Metal Mater. Eng. 32 (2003) 499–503.
[7] K.F. Hsu, S.Y. Tsay, B.J. Hwang, et al., J. Mater. Chem. 14 (17) (2004) 2690–2695.
[8] C. Delacourt, P. Poizot, M. Morcrette, J.M. Tarascon, C. Masquelier, Chem. Mater. 16 (1) (2004) 93.
[9] Y. Iriyama, M. Yokoyama, C. Yada, S.-K. Jeong, I. Yamada, T. Abe, M. Inaba, Z. Ogumi, Eletrochem. Solid-State Lett. 7 (10) (2004) A340–A342.
[10] F. Sauvage, E. Baudrin, M. Morcrette, J.-M. Tarascon, Eletrochem. Solid-State Lett. 7 (1) (2004) A15–A18.
[11] W.C. West, J.F. Whitacre, B.V. Ratnakumar, J. Electrochem. Soc. 150 (2003) A1660.
[12] A. Eftekharo, J. Electrochem. Soc. 151 (9) (2004) A1456–A1460.

[13] W.S. Yoon, S.H. Ban, K.K. Lee, K.B. Kim, M.G. Kim, J.M. Lee, J. Power Sources 97–98 (2001) 282.
[14] D. Shu, K.Y. Chung, W.I. Cho, K.B. Kim, J. Power Sources 114 (2003) 253.
[15] K. Yamada, N. Sato, T. Fujino, C.G. Lee, I. Uchida, J.R. Selman, J. Solid State Electrochem. 3 (1999) 148.
[16] Y.T. Kim, S. Gopukumar, K.B. Kim, B.W. Cho, J. Power Sources 117 (2003) 110.
[17] C.H. Chen, E.M. Kelder, M.J.G. Jak, J. Schoonman, Solid State Ionics 86–88 (1996) 1301–1306.
[18] C.H. Chen, M.H.J. Emond, E.M. Kelder, B. Meester, J. Schoonman, J. Aerosol Sci. 30 (7) (1999) 959.
[19] A. Yamada, S.C. Chung, K. Hinoluma, J. Electrochem. Soc. 148 (2001) A224.
[20] S. Geller, J.L. Dwrand, Acta Crystallogr. 13 (1960) 325.
[21] G. Li, H. Azuma, M. Tohda, Eletrochem. Solid-State Lett. 5 (6) (2002) A135.
[22] S. Okada, S. Sawa, K. Liu, J. Electrochem. Soc. 148 (2001) A1153.
[23] G. Li, H. Azuma, M. Tohda, J. Electrochem. Soc. 149 (6) (2002) A743.
[24] A. Yamada, S.C. Chung, J. Electrochem. Soc. 148 (2001) A960.
[25] A. Yamada, K. Kudo, K.-Y. Liu, J. Electrochem. Soc. 148 (2001) A1153.